Erschienen in: Physical Review Letters ; 117 (2016). - 197202
https://dx.doi.org/10.1103/PhysRevLett.117.197202

Ground-State Cooling of a Mechanical Oscillator by Interference in Andreev Reflection

P. Stadler, W. Belzig, and G. Rastelli
Fachbereich Physik, Universität Konstanz, D 78457 Konstanz, Germany

We study the ground state cooling of a mechanical oscillator linearly coupled to the charge of a quantum dot inserted between a normal metal and a superconducting contact. Such a system can be realized, e.g., by a suspended carbon nanotube quantum dot with a capacitive coupling to a gate contact. Focusing on the subgap transport regime, we analyze the inelastic Andreev reflections which drive the resonator to a nonequilibrium state. For small coupling, we obtain that vibration assisted reflections can occur through two distinct interference paths. The interference determines the ratio between the rates of absorption and emission of vibrational energy quanta. We show that ground state cooling of the mechanical oscillator can be achieved for many of the oscillator's modes simultaneously or for single modes selectively, depending on the experimentally tunable coupling to the superconductor.

Nanoelectromechanical (NEMS) and optomechanical systems promise to manipulate mechanical motion in the quantum regime using, respectively, electrons [1,2] or photons [3], for the realization of fundamental tests of quantum mechanics. This goal requires the mechanical oscillator to be close to the quantum ground state, viz. $T \ll \omega$, with T the temperature and ω the mechanical frequency ($\hbar = k_B = 1$). Ground-state cooling, i.e., the average vibrational quanta $n \ll 1$, has been achieved in some nanomechanical devices, for instance, in an oscillator of gigahertz frequency using standard dilution refrigeration [4]. In another example, ground-state cooling was obtained in an optomechanical setup using the so-called sideband method [5,6], in which one mode of the resonator is coupled to a microwave electromagnetic cavity [7]. Alternatively, several theoretical studies have analyzed proposals for achieving cooling or ground-state cooling using electron transport [8–22]. Most of them are closely related to the mechanism of the sideband cooling [5,6] and are based on an enhanced phonon absorption between two levels of energy difference ΔE. As consequence, cooling is expected when the resonant condition $\omega = \Delta E$ is satisfied.

So far, cooling by electron transport has been experimentally reported in a resonator coupled to a superconducting single-electron transistor [23–25]. Furthermore, suspended carbon nanotube quantum dots (CNTQDs) have proved to be ideal candidates for quantum NEMS [26–28], but the typical frequencies of the relevant modes ($f \lesssim 100$ MHz) correspond to demanding cooling temperatures for electronic circuits [26].

In this Letter, we analyze ground-state cooling of a CNTQD suspended between a normal metal and a superconductor [Fig. 1(a)]. In the subgap transport regime $|eV| \ll \Delta$—with V the voltage and Δ the superconducting gap—we found ground-state cooling due to inelastic Andreev reflections (ARs) [Fig. 1(b)] without the requirement of any resonant condition.

In an AR, an incident electron from the normal contact forms a Cooper pair in the superconductor with the reflection of a hole. Because of the interaction with the mechanical oscillator, ARs can be vibration assisted with the absorption or emission of a vibrational energy quantum or phonon; see Fig. 1(b). For weak coupling, inelastic ARs involve only one phonon at a time and have two possible paths associated with the energy exchange with the resonator before or after an AR; see Fig. 2. These two paths can interfere. Hence, by varying the dot's energy level, we can achieve destructive interference between the paths associated to the phonon emission [Fig. 2(b)] such that the resonator is cooled, since the ARs with phonon absorption dominate [Fig. 2(a)]. This destructive interference can occur in a wide frequency range, which allows us to achieve simultaneous ground-state cooling of multiple mechanical modes.

Model.—We consider the Hamiltonian $\hat{H} = \hat{H}_n + \hat{H}_t + \hat{H}_{dS} + \hat{H}_m$. The part of the normal lead and its tunnel coupling with the quantum dot reads $\hat{H}_n + \hat{H}_t = \sum_{k\sigma}[(\varepsilon_k - eV)\hat{c}^\dagger_{k\sigma}\hat{c}_{k\sigma} + (t_n\hat{d}^\dagger_\sigma\hat{c}_{k\sigma} + \text{H.c.})]$ with $\hat{c}_{k,\sigma}$ and $\hat{d}_\sigma$ the annihilation operators for the electronic states k

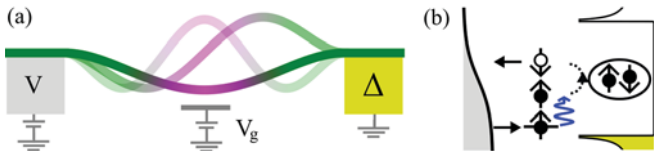

FIG. 1. (a) Suspended CNTQD between a normal lead and a superconductor with a coupling between the dot's charge and the flexural mechanical modes. (b) Example of an inelastic AR: An incoming electron absorbs one phonon from the resonator (blue arrow) before being reflected as a hole.

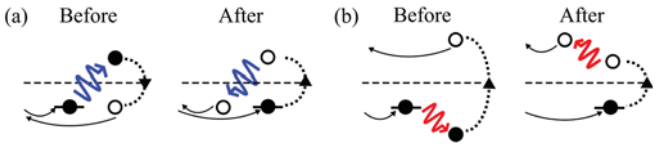

FIG. 2. Inelastic ARs for an incoming electron from the normal lead with the dot's energy below the Fermi level of the superconductor ($\mu = 0$) (dashed line). (a) The two possible paths in which the electron absorbs a phonon (blue arrow) *before* or *after* the AR (dotted line). (b) The two possible paths for the electron emitting a phonon (red arrow).

and spin σ in the normal lead and in the dot, respectively. The tunneling rate is $\Gamma_n = \pi\rho_n|t_n|^2$ with ρ_n the density of states. Elastic as well as inelastic tunneling of quasiparticles above the gap can be neglected in the deep subgap regime $|eV| \ll \Delta$, as their contribution is exponentially small in Δ/T for $T \ll \Delta$ (see Supplemental Material [29] and Ref. [30]). Therefore, we study the following effective Hamiltonian for the dot: $\hat{H}_{dS} = \sum_\sigma \varepsilon_0 \hat{d}^\dagger_\sigma \hat{d}_\sigma - \Gamma_s(\hat{d}^\dagger_\uparrow \hat{d}^\dagger_\downarrow + \hat{d}_\downarrow \hat{d}_\uparrow)$ with ε_0 the dot's energy for two spin-degenerate levels and Γ_s the coupling strength for the intradot pairing due to the proximity with the superconductor. The eigenstates of $\hat{H}_{dS}$ correspond to Andreev states formed by the coherent superposition of electrons and holes with energies $\pm E_A = \pm\sqrt{\varepsilon_0^2 + \Gamma_s^2}$ [31].

In a suspended CNTQD, the electrostatic force between the nanotube and the gate leads to a capacitive coupling between the flexural modes and the dot's charge [26]. Expanding the electrostatic energy in terms of the tube's transversal displacement and the average dot's charge leads to a Holstein interaction $\hat{H}_m = \sum_k [\omega_k \hat{b}^\dagger_k \hat{b}_k + \lambda_k(\hat{b}_k + \hat{b}^\dagger_k)\hat{n}_d]$ with $\hat{b}_k$ the bosonic annihilation operators for the flexural modes ($k = 1, 2, \ldots$) of frequency ω_k and n_d the fluctuating part of the charge [32,33]. Assuming weak coupling, one can neglect the effects of the resonator on the electron system in a first approximation. Then we can analyze the electromechanical damping rate γ and the nonequilibrium phonon occupation number n due to the charge tunneling, separately for each mechanical mode. In the next two sections, we discuss the single-mode case.

Damping for a single mode.—We found that the electromechanical damping is determined by inelastic ARs and normal reflections (NRs). Detailed calculations are reported in Ref. [29]. For the damping rate, we obtain the result $\gamma = \gamma_{\rm AR} + \gamma_{\rm NR}$ in which, for instance, the damping associated to the ARs reads

$$\gamma_{\rm AR} = \gamma^+_{eh} + \gamma^+_{he} - \gamma_{eh} - \gamma_{he}. \tag{1}$$

The individual rates γ^s_{eh} and γ^s_{he} in Eq. (1) correspond to an inelastic AR with the absorption $s = +$ or emission $s = -$ of one phonon for an incoming electron from the normal lead (eh) or an incoming hole (he). As an example, the rates for an electron reflected as a hole (eh) take the form

$$\gamma^\pm_{eh} = \frac{\lambda^2\Gamma_n^2}{2}\int \frac{d\varepsilon}{2\pi} f_e(\varepsilon)[1 - f_h(\varepsilon \pm \omega)]|A_\pm(\varepsilon) + B_\pm(\varepsilon)|^2, \tag{2}$$

with λ the charge-vibration coupling constant and the Fermi functions $f_e(\varepsilon) = \{1 + \exp[(\varepsilon - eV)/T]\}^{-1}$ for the electrons and $f_h(\varepsilon) = 1 - f_e(-\varepsilon)$ for the holes. Hereafter, to be definite, we consider $eV > 0$ and the high-voltage limit, namely, $eV \gg T$, ω, E_A. In this case the rates of the reflections for incoming holes are negligible compared to the ones associated to electrons (vice versa for $eV < 0$), and we approximate $\gamma_{\rm AR} \simeq \gamma^+_{eh} - \gamma_{eh}$. Moreover, we can approximate $f_e \simeq 1$ and $f_h \simeq 0$ in Eq. (2). Hence, the behavior of the rates $\gamma^\pm_{eh}$ is ruled solely by the last term inside the integral Eq. (2) that represents the transmission for inelastic ARs of an incoming electron. The transmission is given by the coherent sum of two amplitudes that are associated to the two possible paths in which the phonon is emitted or absorbed before ($B_\pm$) or after ($A_\pm$) a single AR (Fig. 2) (see also [29]).

Phonon occupation due to inelastic ARs.—We first analyze the contribution of inelastic ARs to the phonon occupation assuming that NRs are negligible. In this case, we find the result

$$n = n_{\rm AR} \equiv \frac{1}{\kappa - 1}, \qquad \kappa = \frac{\gamma^+_{eh}}{\gamma_{eh}} \simeq \frac{(\varepsilon_0 - \omega/2)^2 + \Gamma_n^2}{(\varepsilon_0 + \omega/2)^2 + \Gamma_n^2}, \tag{3}$$

valid for $\kappa > 1$. Thus, $n_{\rm AR}$ is the outcome of the competition between emission and absorption processes for inelastic ARs: For $\kappa \gg 1$, the resonator can be cooled to the ground state with $n_{\rm AR} \ll 1$, whereas the phonon occupation is increased for $\kappa \gtrsim 1$ such that $n_{\rm AR} \gg 1$. Eventually, the resonator is unstable for $\kappa < 1$ [21]. The different regimes can be reached only by tuning the dot's energy level ε_0 (i.e., the gate voltage): $n_{\rm AR} > 1$ and the instability always occurs for $\varepsilon_0 > 0$, whereas $n_{\rm AR} < 1$ is achieved as long as $\varepsilon_0 < 0$. In particular, the lowest phonon occupation is given by $n_{\rm opt} = (\Gamma_n/\omega)^2$ corresponding to ground-state cooling for $\Gamma_n \ll \omega$ [28].

It is interesting to analyze the behavior of the individual rates as a function of ω (Fig. 3). Focusing on the regime $\varepsilon_0 < 0$, the condition $\kappa \gg 1$ for the ground-state cooling occurs either in the limit $\Gamma_s \ll |\varepsilon_0|$ when γ^+_{eh} has a peak [Fig. 3(a)] or in the limit $\Gamma_s \gg |\varepsilon_0|$ when γ_{eh} has a broadened depletion around a dip [Fig. 3(b)].

The peak in Fig. 3(a) results from a resonance: The reflected hole is injected at the same energy as the incoming electron $\varepsilon_0 = -\omega/2$ in the case of phonon absorption [Fig. 2(a)]. This energy alignment holds independently whether the absorption occurs after or before an AR and enhances the phonon absorption amplitudes. Such an

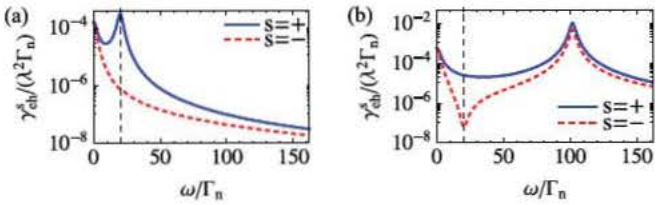

FIG. 3. The rates $\gamma^{\pm}_{eh}$ for inelastic ARs for $\varepsilon_0 = -10\Gamma_n$ ($s = +$, absorption; $s = -$, emission). The vertical dashed line is $\omega = 2|\varepsilon_0|$. (a) Weak coupling regime between the dot and the superconductor with $\Gamma_s = 0.1|\varepsilon_0|$. (b) Strong coupling regime with $\Gamma_s = 5|\varepsilon_0|$.

alignment does not occur for ARs with phonon emission [Fig. 2(b)].

In contrast, the dip of the emission rate in Fig. 3(b) occurs because the two paths with phonon emission in Fig. 2(b) interfere destructively, $|A \quad + B \ | \ll |A \ |, |B \ |$ as mentioned earlier, and the resonator is cooled due to the absorption process, namely, $|A_+ + B_+| \gg |A \quad + B \ |$. The latter condition occurs even when the moduli of all the amplitudes are of the same order of magnitude. Eventually, increasing the frequency, the two rates become comparable $\gamma^+_{eh} \sim \gamma_{eh}$ and both rates show a peak at $\omega \simeq 2\Gamma_S$ [Fig. 3(b)] corresponding to the energy separation between the two Andreev levels ($E_A \simeq \Gamma_s$). However, for $|\varepsilon_0| \lesssim \omega \lesssim \Gamma_S$, we notice γ_{eh} is still 2 orders of magnitudes smaller than γ^+_{eh} [Fig. 3(b)]. This suppression of the emission rate for an inelastic AR in a wide frequency range allows us to cool many mechanical modes of different frequency. The extension of this suppression sets approximately the cooling spectral band.

Such an interference mechanism of cooling is different from the method based on the quasiparticle transport involving inelastic tunneling with electronic states above the gap [34–36]. Inelastic quasiparticles and Andreev transport for heating has been discussed in Ref. [37], although subgap ground-state cooling was not studied. Cooling by interference was also discussed in Ref. [38] but by using a dissipative optomechanical coupling.

General results and effects of the normal reflections.—Formally, the electromechanical damping γ and the steady nonequilibrium phonon occupation n are determined by the spectrum of the nonsymmetrized noise of the dot's charge occupation $S(\varepsilon) = \int dt e^{i\varepsilon t}\langle \hat{n}_d(t)\hat{n}_d\rangle$, where the quantum statistical average is taken over the electron system [39]. Explicit relations between γ, n, and the noise $S(\varepsilon)$ are given in Ref. [29]. For the phonon occupation, we obtain

$$n = \frac{\gamma_{\rm AR} n_{\rm AR} + (\gamma_{\rm NR} + \gamma_0) n_B(\omega)}{\gamma_{\rm AR} + \gamma_{\rm NR} + \gamma_0}, \tag{4}$$

with the Bose function $n_B(\omega) = [\exp(\omega/T) - 1]^{-1}$ and an intrinsic damping $\gamma_0 = \omega/Q$, with the quality factor $Q \sim 10^6$ [26,27]. The NRs that involve only the normal lead at the bath temperature can drive the oscillator only towards thermal equilibrium. The general expression for $n_{\rm AR}$ reads

$$n_{\rm AR} = \sum_{s=\pm} [\gamma^s_{eh} n_B(\omega + s2eV) + \gamma^s_{he} n_B(\omega - s2eV)]/\gamma_{\rm AR}. \tag{5}$$

An example of the result for n is shown in Fig. 4(a) for some realistic parameters. Restoring the NRs in the phonon occupation increases the minimum occupation attainable by ARs. However, we obtain $n_{\rm min} \simeq 0.05$ in the region $\varepsilon_0 < 0$ of Fig. 4(a); i.e., ground state cooling is still feasible. In the region of the dot's level $\varepsilon_0 > 0$, the situation in Fig. 4(a) is inverted: The emission rates of the inelastic ARs dominates over the absorption ones, leading to an increase of the phonon occupation (in the region of stability $\gamma_{\rm AR} + \gamma_{\rm NR} + \gamma_0 > 0$) and eventually to a mechanical instability.

When we take into account NRs, the minimal occupation becomes a function of Γ_s and there is an optimal value for the coupling with the superconducting lead that maximizes the cooling, as shown in Fig. 4(b). Setting $\varepsilon_0 = -\omega/2$ and $eV \gg (\omega, T)$, in the limit of small intrinsic damping $\gamma_0 \ll \gamma_{\rm NR}$ and for strong suppression of the phonon emission rate $\gamma_{eh} \ll \gamma^+_{eh}$ ($n_{\rm opt} \ll 1$), we have $n_{\rm min} \approx [\gamma^+_{eh} n_{\rm opt} + \gamma_{\rm NR} n_B(\omega)]/(\gamma^+_{eh} + \gamma_{\rm NR})$. For $\Gamma_s \to 0$, we have $\gamma^+_{eh} \to 0$, NRs dominate over ARs, and the oscillator is close to the thermal equilibrium. Increasing Γ_s, the resonator starts to be cooled due to the ARs and the phonon occupation approaches the optimal value $n_{\rm opt}$. As the AR rate γ^+_{eh} vanishes at large Γ_s (see Fig. 3), $n_{\rm min}$ shows a nonmonotonic behavior.

Results for several mechanical modes.—In this section, we illustrate the possibility of cooling several nondegenerate mechanical modes owing to the interference between the inelastic ARs paths with phonon emission.

We assume a low-frequency spectrum $\omega_k = k\omega$ (i.e., under sufficiently high tension). We limit the calculations

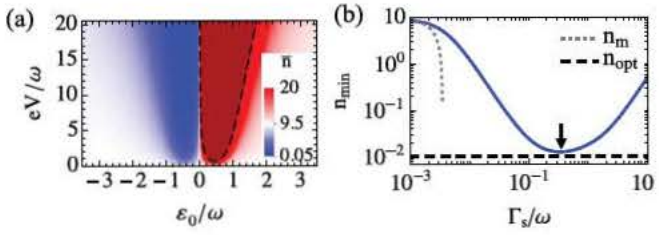

FIG. 4. (a) Phonon occupation as a function of V and ε_0 for $\Gamma_s = 0.35\omega$. White corresponds to $n_B(\omega)$. The dark red region limited by the dashed line corresponds to the instability region $\gamma_{\rm AR} + \gamma_{\rm NR} + \gamma_0 < 0$. (b) Minimal phonon occupation as a function of Γ_s for $\varepsilon_0 = -\omega/2$. The lowest possible occupation is $n_{\rm opt} = (\Gamma_n/\omega)^2$ (dashed black line). The dotted line (gray) is the analytic approximation $n_m \approx n_B(\omega)[1 - 8\pi\Gamma_s^2/(\Gamma_n\gamma_{\rm NR})]$ for $\Gamma_s \ll \omega$; see also [29]. The arrow points the optimal point at $\Gamma_s = 0.35\omega$. Parameters: $\Gamma_n = 0.1\omega$, $T = 10\omega$, $\gamma_0/\omega = 10^{-6}$, and $\lambda = 0.1\omega$ [33].

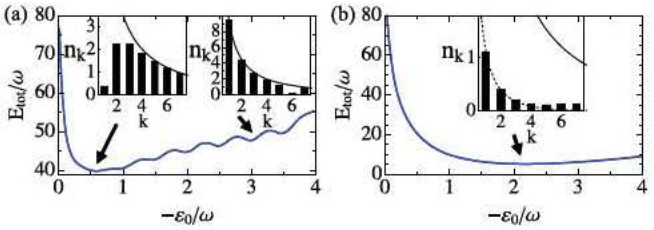

FIG. 5. The total mechanical energy with $N = 7$ modes at $eV = 16\omega$ for $\Gamma_s = 0.1\omega$ (a) and $\Gamma_s = 5\omega$ (b). The insets show the occupation of each mode k at specific points of ε_0 specified by the arrows. The solid black line shows the thermal distribution $n_B(\omega_k)$. The dashed line in the inset (b) is the Bose distribution $n_B^*(\omega_k)$ with $T^* = 1.6\omega$. Parameters: $\Gamma_n = 0.1\omega$ and $T = 10\omega$.

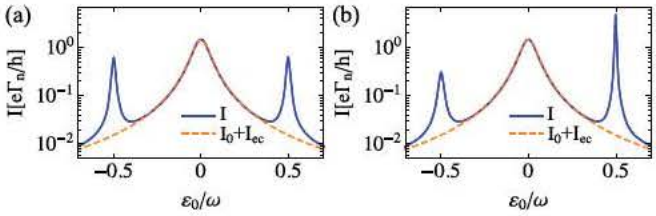

FIG. 6. Total current I (solid blue line) and elastic current (dashed orange line) as a function of ε_0. In (a), the case of the thermal equilibrated oscillator $\bar{n} = n_B$. In (b), the oscillator is in a nonequilibrium state with $\lambda = 0.02\omega$ and $\gamma_0/\omega = 10^{-4}$. The ratio between the areas underlying the two peaks is related to the phonon occupation. Parameters: $\Gamma_n = 0.01\omega$, $\Gamma_s = 0.04\omega$, $T = 10\omega$, and $eV = 5\omega$.

by considering a finite number of modes, as we have a natural cutoff given by the temperature: High-frequency modes with $\omega_k \gtrsim T$ are close to the ground state. As an example, in Fig. 5, we show the result for the total mechanical energy defined as $E_{\rm tot} = \sum_{k=1}^{7} \omega_k n_k$ for the case for $T = 10\omega$ and $N = 7$ modes. The nonequilibrium value n_k for each mode is calculated by Eq. (4) for $\gamma_0 \ll \gamma_{\rm NR}$.

In Fig. 5(a), we consider the regime of weak coupling between the dot and the superconductor ($\Gamma_s \ll \omega_k$), namely, the regime of cooling by resonance. In this case, by matching the resonance condition $2|\varepsilon_0| = \omega_k$, one can obtain cooling of each individual mode, as, for instance, for $k = 1$ or $k = 6$, whereas the rest of the modes are approximately at the thermal equilibrium.

In Fig. 5(b), we consider the regime of strong coupling between the dot and the superconductor ($\Gamma_s \gg \omega_k$), namely, the regime of cooling by interference. In this case, several modes of the resonator can be cooled close to the ground state simultaneously. Notice that the nonequilibrium distribution of the modes does not correspond to $n_B^*(\omega_k)$ with a common effective temperature T^* [e.g., see the tail of the fitting curve in the inset in Fig. 5(b)]. Indeed, the phonon occupation for each mode n_k is an interpolation (with frequency-dependent coefficients) between $n_B(\omega_k)$ resulting from NRs and the algebraic function $n_{\rm AR} \sim n_{\rm opt} = \Gamma_n^2/\omega_k^2$ resulting from ARs.

dc current.—We discuss as an example the results for a single mode. To lowest order in the charge-vibration coupling λ, the current can be expressed as $I = I_0 + I_{\rm ec}(\lambda^2) + I_{\rm in}(\lambda^2)$, with the elastic current I_0, the elastic correction $I_{\rm ec}$, and the inelastic current $I_{\rm in}$. Figure 6 shows the current at $eV = 5\omega$ as a function of ε_0. Beyond a peak at $\varepsilon_0 = 0$ associated to $I_0 + I_{\rm ec}$, two vibrational peaks appear at $\varepsilon_0 = \pm\omega/2$ associated to $I_{\rm in}$: They correspond to inelastic ARs with emission or absorption of one phonon. Similar vibrational sidebands have been observed for molecular vibrational modes but under the condition $T < \omega$ (for instance, in suspended CNTQDs; see Refs. [40–42]) and in other nonsuspended devices due to other bosonic modes of the environment [43]. In our case, these peaks are visible in the subgap transport even for the temperature of the leads $T \gg \omega$. Analytic expressions for the I_0 and $I_{\rm ec}$ are given in Ref. [29]; here we focus on $I_{\rm in}$.

As shown in Fig. 6, around the region $\varepsilon_0 = \pm\omega/2$ the main contribution to the current is given by the inelastic component, which reads

$$I_{\rm in}/e = [n\gamma_{eh}^{+} + (n+1)\gamma_{eh}] - [n\gamma_{he}^{+} + (n+1)\gamma_{he}]. \qquad (6)$$

For instance, for positive $eV > 0$ and a high-voltage limit, the first term of the right-hand side of Eq. (6) is the leading one, and it is associated to the flux of the incoming electrons, as discussed previously. For $\gamma_0 \gg \gamma$, $n \simeq n_B(\omega)$ and the peaks are approximately symmetric [Fig. 6(a)]. In the opposite case $\gamma_0 \ll \gamma$, the oscillator is in the nonequilibrium state as given by Eq. (4) and the two peaks are strongly asymmetric [Fig. 6(b)]. Integrating the peaks separately over ε_0 (see Ref. [29]), we can extract information about the phonon occupation by the ratio $\rho = \Delta I_l/\Delta I_r \approx (2n_l + 1)/(2n_r + 1)$, where $\Delta I_{l,r}$ are the approximated integrals of the left and right peaks, respectively, in Fig. 6 and n_l and n_r are the phonon occupations around such peaks.

One can verify the nonequilibrium state of the resonator in different ways. For example, one can vary the voltage and calculate $\rho(eV)$ for each point: At a low voltage the resonator is close to the thermal state with $\rho \simeq 1$, whereas at a high voltage one expects $\rho \ll 1$. Alternatively, one can tune the coupling Γ_s with the superconductor, as in the experimental setup of Ref. [28]. Finally, when many mechanical modes are considered, several peaks appear in the inelastic current—with broadening controlled by Γ_n [31]—and one can repeat the same procedure for determining $\rho(\omega_k)$ associated to each mode k.

Conclusions.—We discussed the ground-state cooling due to inelastic ARs for a mechanical resonator coupled to a quantum dot. We showed that the destructive interference in the ARs with phonon emission allows for the cooling of several mechanical modes. Our proposal is well within the

reach of the state of art for carbon-based NEMS. The setup with hybrid contacts in Fig. 1(a) can be experimentally implemented [43,44] as well as the strong electromechanical coupling regime for flexural modes [28,45–47] such that the intrinsic damping γ_0 is much smaller than the electromechanical one $\gamma_0 \ll \gamma$.

We acknowledge A. Armour for interesting discussions and for a critical reading of the manuscript. We also thank S. Girvin, A. K. Huettel, and A. Bachtold for useful comments. This research was supported by the Zukunftskolleg of the University of Konstanz and by the DFG through the collaborative research center SFB 767.

[1] M. Poot and H. S. J. van der Zant, Phys. Rep. **511**, 273 (2012).
[2] Y. S. Greenberg, Y. A. Pashkin, and E. Il'ichev, Usp. Fiz. Nauk **182**, 407 (2012).
[3] M. Aspelmeyer, T. J. Kippenberg, and F. Marquardt, Rev. Mod. Phys. **86**, 1391 (2014).
[4] A. D. O'Connell, M. Hofheinz, M. Ansmann, R. C. Bialczak, M. Lenander, E. Lucero, M. Neeley, D. Sank, H. Wang, M. Weides, J. Wenner, J. M. Martinis, and A. N. Cleland, Nature (London) **464**, 697 (2010).
[5] F. Marquardt, J. P. Chen, A. A. Clerk, and S. M. Girvin, Phys. Rev. Lett. **99**, 093902 (2007).
[6] T. J. Kippenberg and K. J. Vahala, Science **321**, 1172 (2008).
[7] J. D. Teufel, T. Donner, D. Li, J. W. Harlow, M. S. Allman, K. Cicak, A. J. Sirois, J. D. Whittaker, K. W. Lehnert, and R. W. Simmonds, Nature (London) **475**, 359 (2011).
[8] I. Martin, A. Shnirman, L. Tian, and P. Zoller, Phys. Rev. B **69**, 125339 (2004).
[9] U. Lundin, Phys. Lett. A **332**, 127 (2004).
[10] D. A. Rodrigues, J. Imbers, and A. D. Armour, Phys. Rev. Lett. **98**, 067204 (2007).
[11] K. R. Brown, J. Britton, R. J. Epstein, J. Chiaverini, D. Leibfried, and D. J. Wineland, Phys. Rev. Lett. **99**, 137205 (2007).
[12] F. Xue, Y. D. Wang, Y. x. Liu, and F. Nori, Phys. Rev. B **76**, 205302 (2007).
[13] F. Pistolesi, J. Low Temp. Phys. **154**, 199 (2009).
[14] S. Zippilli, G. Morigi, and A. Bachtold, Phys. Rev. Lett. **102**, 096804 (2009).
[15] M. Galperin, K. Saito, A. V. Balatsky, and A. Nitzan, Phys. Rev. B **80**, 115427 (2009).
[16] G. Sonne, M. E. Peña Aza, L. Y. Gorelik, R. I. Shekhter, and M. Jonson, Phys. Rev. Lett. **104**, 226802 (2010).
[17] F. Santandrea, L. Y. Gorelik, R. I. Shekhter, and M. Jonson, Phys. Rev. Lett. **106**, 186803 (2011).
[18] Z. Z. Li, S. H. Ouyang, C. H. Lam, and J. Q. You, Europhys. Lett. **95**, 40003 (2011).
[19] G. Sonne and L. Y. Gorelik, Phys. Rev. Lett. **106**, 167205 (2011).
[20] P. Stadler, W. Belzig, and G. Rastelli, Phys. Rev. Lett. **113**, 047201 (2014).
[21] P. Stadler, W. Belzig, and G. Rastelli, Phys. Rev. B **91**, 085432 (2015).
[22] L. Arrachea, N. Bode, and F. von Oppen, Phys. Rev. B **90**, 125450 (2014).
[23] A. Naik, O. Buu, M. D. LaHaye, A. D. Armour, A. A. Clerk, M. P. Blencowe, and K. C. Schwab, Nature (London) **443**, 193 (2006).
[24] M. P. Blencowe, J. Imbers, and A. D. Armour, New J. Phys. **7**, 236 (2005).
[25] A. A. Clerk and S. Bennett, New J. Phys. **7**, 238 (2005).
[26] A. K. Hüttel, G. A. Steele, B. Witkamp, M. Poot, L. P. Kouwenhoven, and H. S. J. van der Zant, Nano Lett. **9**, 2547 (2009).
[27] J. Moser, A. Eichler, J. Güttinger, M. I. Dykman, and A. Bachtold, Nat. Nanotechnol. **9**, 1007 (2014).
[28] A. Benyamini, A. Hamo, S. V. Kusminskiy, F. von Oppen, and S. Ilani, Nat. Phys. **10**, 151 (2014).
[29] See Supplemental Material at http://link.aps.org/supplemental/10.1103/PhysRevLett.117.197202 for details of the calculation.
[30] J. C. Cuevas, A. Martín Rodero, and A. Levy Yeyati, Phys. Rev. B **54**, 7366 (1996).
[31] Note that the coupling Γ_s to the superconductor does not produce any broadening.
[32] S. Braig and K. Flensberg, Phys. Rev. B **68**, 205324 (2003).
[33] G. Rastelli, M. Houzet, L. Glazman, and F. Pistolesi, C. R. Phys. **13**, 410 (2012).
[34] F. W. J. Hekking, A. O. Niskanen, and J. P. Pekola, Phys. Rev. B **77**, 033401 (2008).
[35] P. J. Koppinen and I. J. Maasilta, Phys. Rev. Lett. **102**, 165502 (2009).
[36] A. V. Feshchenko, L. Casparis, I. M. Khaymovich, D. Maradan, O. P. Saira, M. Palma, M. Meschke, J. P. Pekola, and D. M. Zumbühl, Phys. Rev. Applied **4**, 034001 (2015).
[37] Q. Wang, H. Xie, H. Jiao, and Y. H. Nie, Europhys. Lett. **101**, 47008 (2013).
[38] F. Elste, S. M. Girvin, and A. A. Clerk, Phys. Rev. Lett. **102**, 207209 (2009).
[39] A. A. Clerk, Phys. Rev. B **70**, 245306 (2004).
[40] R. Leturcq, C. Stampfer, K. Inderbitzin, L. Durrer, C. Hierold, E. Mariani, M. G. Schultz, F. von Oppen, and K. Ensslin, Nat. Phys. **5**, 327 (2009).
[41] B. J. LeRoy, S. G. Lemay, J. Kong, and C. Dekker, Nature (London) **432**, 371 (2004).
[42] S. Sapmaz, P. Jarillo Herrero, Y. M. Blanter, C. Dekker, and H. S. J. van der Zant, Phys. Rev. Lett. **96**, 026801 (2006).
[43] J. Gramich, A. Baumgartner, and C. Schönenberger, Phys. Rev. Lett. **115**, 216801 (2015).
[44] J. Schindele, A. Baumgartner, R. Maurand, M. Weiss, and C. Schönenberger, Phys. Rev. B **89**, 045422 (2014).
[45] G. A. Steele, A. K. Huttel, B. Witkamp, M. Poot, H. B. Meerwaldt, L. P. Kouwenhoven, and H. S. J. van der Zant, Science **325**, 1103 (2009).
[46] B. Lassagne, Y. Tarakanov, J. Kinaret, D. Garcia Sanchez, and A. Bachtold, Science **325**, 1107 (2009).
[47] A. Eichler, M. del Álamo Ruiz, J. A. Plaza, and A. Bachtold, Phys. Rev. Lett. **109**, 025503 (2012).